EVALUATING HIGH-RESOLUTION NWP MODELS USING KINETIC ENERGY SPECTRA

William C. Skamarock[1], Michael E. Baldwin[2], and Wei Wang[1]

[1]National Center for Atmospheric Research*
Boulder, Colorado

[2]NOAA/National Severe Storms Laboratory
Norman, Oklahoma

The atmospheric kinetic energy spectra in the free troposphere and lower stratosphere possess a robust and remarkable universality. Results from an observational analysis of kinetic energy spectra, produced in a seminal study by Nastrom and Gage (1985) using the GASP (Global Atmospheric Sampling Program) dataset, are shown in Figure 1. The spectrum in figure 1 illustrates the large-scale k^{-3} dependence of the atmospheric kinetic energy spectrum, along with a transition to a shallower $k^{-5/3}$ dependence found in the mesoscale and smaller scales. Also depicted in Figure 1 is the result of an analysis of the MOZAIC (Measurement of Ozone and Water Vapor by Airbus In-Service Aircraft) aircraft observations by Lindborg (1999). Making use of structure functions, Lindborg produced a simple functional fit to the MOZAIC kinetic energy spectrum that results in a remarkably close fit to the GASP kinetic energy spectrum. These and other results have shown very little dependence on latitude, season, or altitude.

Atmospheric models should be able to reproduce the observed kinetic energy spectrum. Global forecast models and climate models generally reproduce the large-scale k^{-3} spectral character, and the spectra are regularly used to examine filter formulations (e.g. Laursen and Eliasen, 1989). At small scales, cloud model simulations of convection have been evaluated using kinetic energy spectra. Convective simulations clearly show a shallow spectral slope of approximately -5/3 (e.g. Vallis et al, 1997), in addition to showing that the kinetic energy is dominated by the kinetic energy associated with divergent modes, as opposed to the dominance of the rotational energy at the large scales.

In this brief abstract we show that forecasts produced by the WRF ARW core for the BAMEX (Bow Echo and Mesoscale Vortices Experiment) 2003 field campaign reproduce the observed spectra. We examine the spinup of the spectra and the effective model resolution as revealed by the spectra. We also show examples of spectra from MM5, COAMPS, NCEP-NMM, and the operational NCEP-Eta model.

Corresponding author address: Dr. William C. Skamarock, NCAR, P.O. Box 3000, Boulder, CO 80307-3000. email: *skamaroc@ucar.edu*
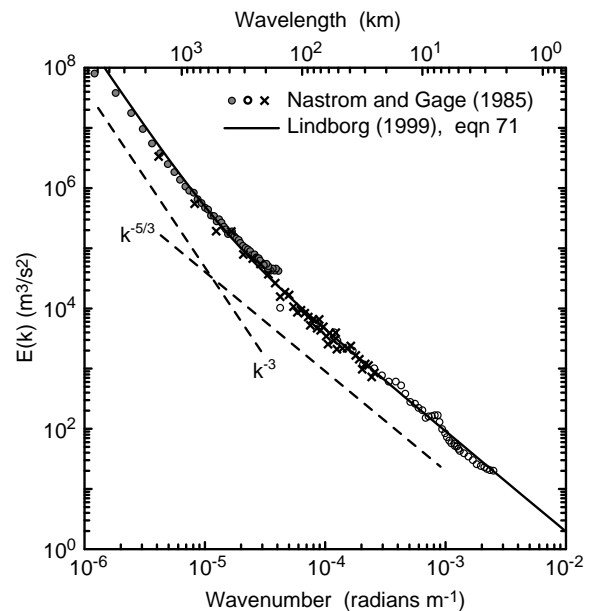
Figure 1. Nastrom and Gage (1985) spectrum derived from the GASP aircraft observations (symbols) and the Lindborg (1999) functional fit to the MOZAIC aircraft observations.

1. WRF-BAMEX SPECTRA

In the BAMEX field campaign (Davis et al, 2004) that occurred between mid-May and early July 2003, the WRF model was used to produce daily 36 h forecasts using grids with horizontal grid spacing of 22, 10 and 4 km beginning at 0Z each day (there were also 12Z forecasts that we do not examine here). The forecast domains were centered over the central US and the model configurations are described in Done et al (2004). The late-spring/early-summer BAMEX period was convectively active, with an average of two to three long-lived convective systems occurring within the field program (and forecast) domain per day (Done et al, 2004). There were generally some weak-to-moderate synoptic-scale waves traversing the region, most often in the northern or central latitudes of the forecast domains.

We have computed kinetic energy spectra from the 4 km BAMEX forecasts for the entire forecast period (daily 36 h forecasts initialized at 0Z from 5
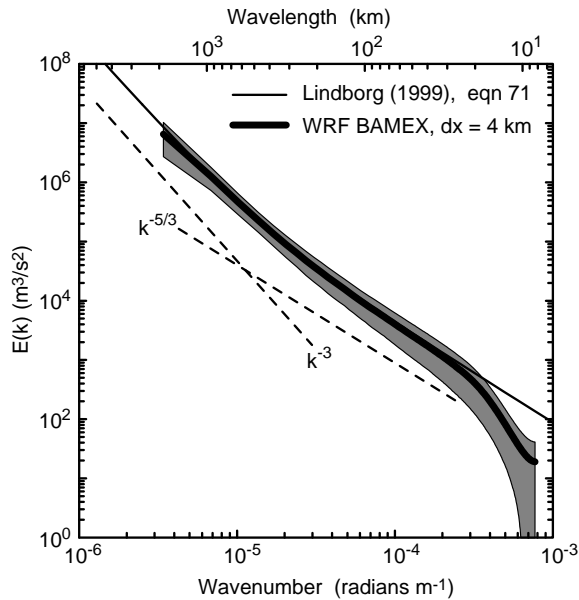
Figure 2. Spectra from the 4 km WRF BAMEX forecasts from 5 May 2003 to 14 July 2003. The shaded area encloses plus/minus one standard deviation. The Lindborg (1999) functional fit to the MOZAIC aircraft observations is also plotted.
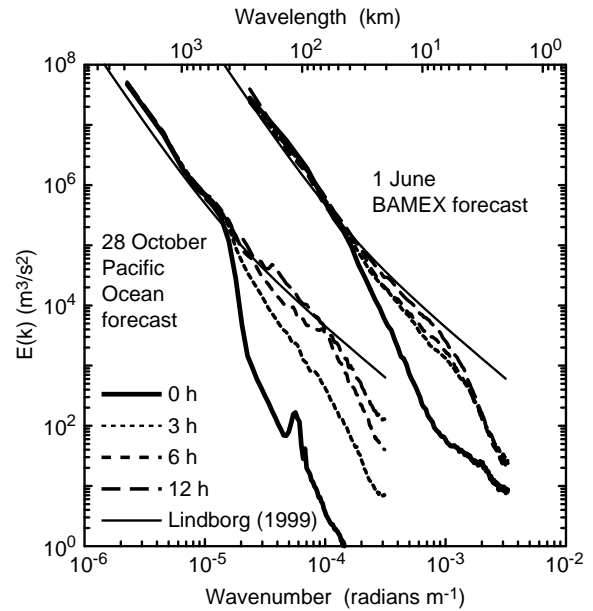

Figure 3. Spin-up of the WRF model spectra for an autumn forecast over the north-central Pacific Ocean (left) and the 1 June BAMEX forecast (right). The Pacific forecast is initialized from an 80 km GFS analysis, and the BAMEX forecast is initialized with a 40 km Eta analysis. The BAMEX forecast spectra are shifted one decade to the right for clarity.

May 2003 through 14 July 2003). Figure 2 shows the time-averaged spectrum and its standard deviation for this forecast period along with the Lindborg (1999) functional fit to the MOZAIC spectrum. The 4 km forecast spectrum follows the Lindborg spectrum very well, indicating that the forecast spectrum follows the MOZAIC observations and the GASP observations of Nastrom and Gage (1985) shown in figure 1. The forecast spectrum has a slope of somewhat less than -3 at large wavelength and transitions to a shallower slope with increasing wavenumber, following the Lindborg (1999) spectrum function down to wavelengths around 30 km. There is significant variance associated with this spectrum as revealed by the magnitude of the standard deviation relative to the energy density depicted in figure 2. The standard deviation is similar in magnitude to the energy density for all wavelengths. This is consistent with the GASP observations as suggested by the spread in the GASP observational spectrum plotted in figure 1.

We have also examined spectra from 10 and 22 km forecasts that we conducted for BAMEX. Similar to the 4 km spectrum shown in figure 2, these forecast spectra show energy levels that are generally of the correct magnitude overall except at the highest wavenumbers, where model dissipation removes energy and depresses the spectra. The 22 km CONUS forecast shows a small indication of a transition in spectral slope from -3 to a shallower slope, while both the 10 and 4 km forecast spectra show clear evidence of the shallower mesoscale regime but little of the k^{-3} regime. The KE spectra for the 10 and 4 km forecasts possess slopes of approximately -2 in the mesoscale, close to the Nastrom and Gage (1985) analysis, similar to the Lindborg (1999) functional fit to the MOZAIC data (figure 1) and consistent with other observations. Further details on the spectra and its computation are given in Skamarock (2004).

2.   SPIN-UP OF THE SPECTRA

The BAMEX forecasts are initialized using coarse-resolution analyses. Given that forecast models must, of necessity, develop the mesoscale KE spectrum on their own, two questions arise: (1) Is the timescale of the development consistent with theory, (2) are the mesoscale phenomena that develop realistic? Figure 3 shows the WRF-mass model forecast spectra for the 1 June BAMEX forecast on the 10 km grid at 0, 3, 6 and 12 h, and for a 28 October forecast over the Pacific Ocean. The spectrum develops quickly, as expected based on theory. Additionally, the mesoscale structures that form appear realistic. Details can be found in Skamarock (2004).

The spin-up period for the mesoscale spectrum and structures is short (hours) relative to the forecast periods (days). The rapid spin-up implies that high-resolution forecasts may have increased value because they may be able to deterministically predict mesoscale structure if correctly forced by the larger scale or by external forcings (e.g., deep convection forced by fronts), or they
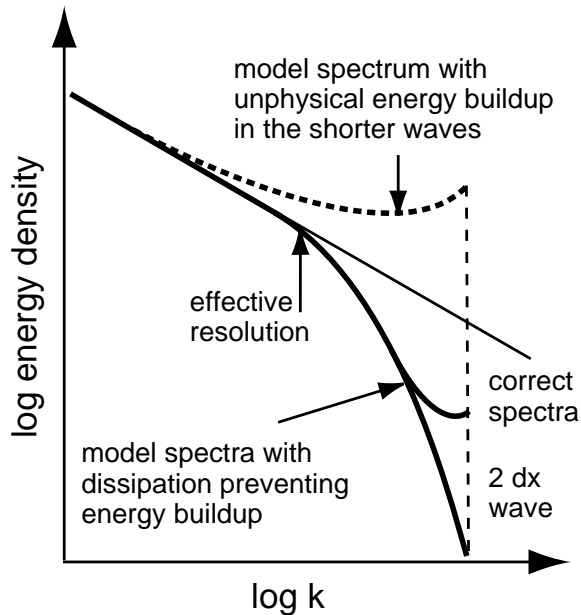
Figure 4. Schematic depicting the possible behavior of spectral tails derived from model forecasts. 1D spectra computed from limited area models (including WRF) usually produce a slightly upturned tail.

Figure 5. Effective resolution determined from forecast-derived spectra for the BAMEX-configured WRF model at 10 and 4 km horizontal grid spacing.

may remove the need for problematic parameterizations (e.g., parameterizations of deep convection).

3. DISSIPATION AND THE KE SPECTRA

The most revealing feature of model KE spectrum are the tails, that is, the high wavenumber portion of the spectrum. Examples of model spectra from the literature and in this paper suggest that three general types of model behavior are common, and these are depicted schematically in figure 4. The first two types (thick solid lines) show the energy density decaying as the grid resolution limit is reached. Model filters remove energy most strongly at the highest wavenumbers, with less energy removal occurring at decreasing wavenumbers (increasing wavelengths). Given that model discretizations typically produce their greatest errors at the smallest wavelengths, the small amount of energy in these modes (relative to what would exist at these wavenumbers) means that there is little energy to be aliased to the longer, well resolved modes. The 1D spectra we have computed on spatially limited domains tend to have a small upturn at the end of the tails, as opposed to the steep decay shown in LES derived spectra or spectra from global models (e.g. Laursen and Eliasen, 1989).

Figure 4 also shows a spectrum where the highest wavenumber modes in an NWP model are poorly handled (thick dashed line) – there is buildup of energy to physically unrealistic levels at the highest wavenumbers. Energy is being reflected (aliased) to
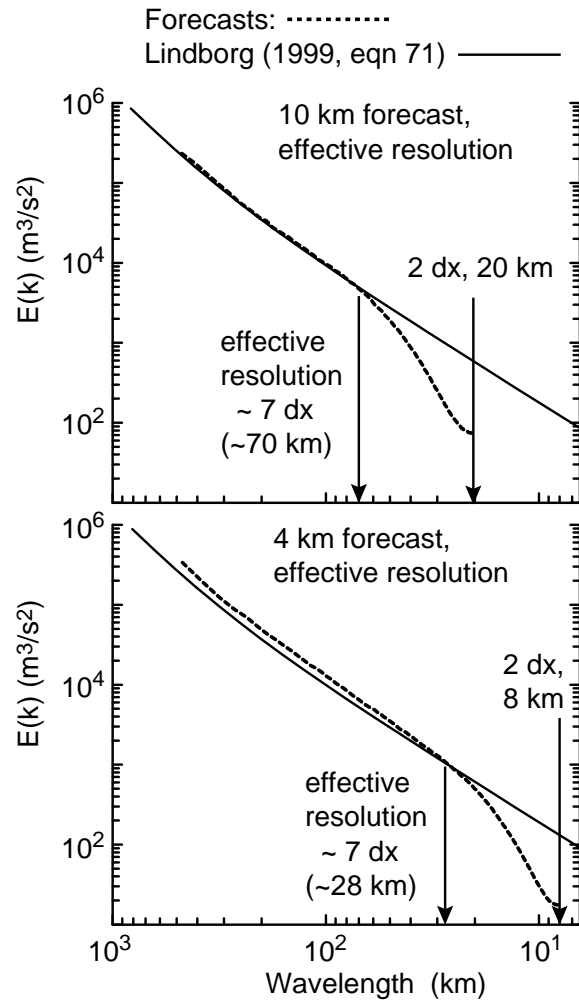
the lower wavenumber modes of the solution and the reflection casts doubt on a considerable portion of the spectrum and the physical phenomena represented by these modes.

The WRF model spectrum presented in figure 2 possesses a spectral tail corresponding to a decaying energy density as the grid-resolution is reached, that is, the WRF model spectral tails are damped and decaying relative to the actual spectra. These results represent our best attempt at a minimal-dissipation configuration of the model. Further reduction of the dissipation in the WRF model would lead to increased energy at the smaller scales and poorer spectral tails.

For the WRF BAMEX simulations, figure 5 reveals that the effective resolution of the WRF model 10 and 4 km configurations, using the 1-3 June forecast spectra (given in figure 2 for the 4 km model), is generally around $7 \Delta x$. The fact the the effective resolution of
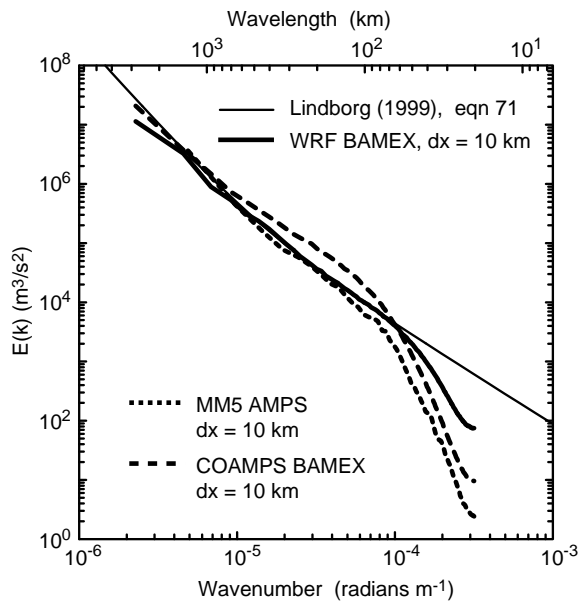
Figure 6. Spectra from MM5 (AMPS), COAMPS-BAMEX and WRF-BAMEX simulations using 10 km horizontal grid spacing.
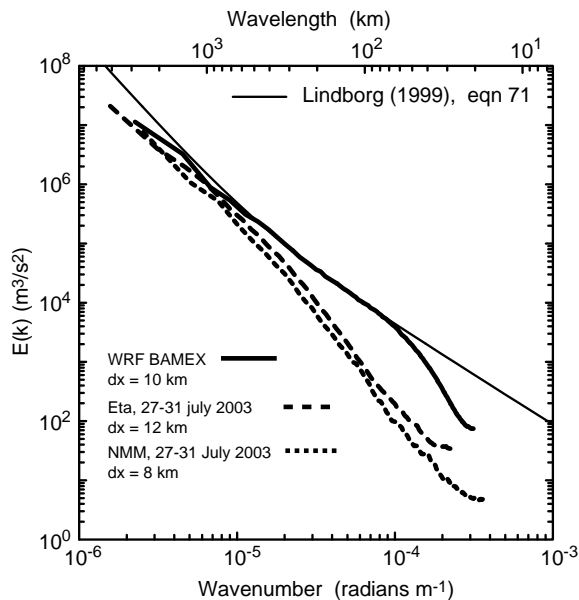

Figure 7. Spectra from the operational Eta, NMM and WRF-BAMEX simulations using 12, 10 and 8 km horizontal grid spacing, respectively.

the WRF model is a constant multiple of Δx is not surprising because the model filters scale with the model grid spacing. Given the problems with phase errors for increasingly shorter wavelengths, we believe that we are close to the limit of the spatial resolving capabilities of finite difference models, particularly those using explicit methods.

4. SPECTRA FROM OTHER MODELS

Spectra from the MM5 model forecasts over Antarctica, and from the COAMPS model forecasts over the BAMEX domain, are depicted in Figure 6. Both model spectra show a steepening spectral slope and the effects of filter beginning at wavelengths of approximately 10 dx. Additionally, the spectra show a significantly more rapid decay at the higher wavenumbers compared to the WRF model.

Spectra from NCEP's operational Eta model and from the NMM are shown in figure 7. The model forecasts are from operational (Eta) and threat-domain (NMM) forecasts for late July 2003 conducted with the model configurations in use at that time. Strong horizontal filtering results in a depression of the spectra over a wide wavenumber range (see Skamarock and Baldwin white paper at *http://www.mmm.ucar.edu/individual/skamarock/ spectra_discussion.html* for further information). More recently, the WRF NMM core has been tested using significantly reduced horizontal filtering. We will show spectra from these tests at the workshop if they are available.

5. REFERENCES

Davis, C. and co-authors, 2004: The Bow-Echo and MCV Experiment (BAMEX): Observations and Opportunities. *Bull. Amer. Meteorol. Soc.,* submitted.

Done, J., C. Davis and M. Weisman, 2004: The next generation of NWP: Explicit forecasts of convection using the Weather Research and Forecast (WRF) model. *Atmos. Sci. Lett.,* submitted.

Koshyk, J. N., and K. Hamilton, 2001: The horizontal kinetic energy spectrum and spectral budget simulated by a high-resolution troposphere-stratosphere-mesosphere GCM. *J. Atmos. Sci.,* **58,** 329-348.

Laursen, L. and E. Eliasen, 1989: On the effects of the damping mechanisms in an atmospheric general circulation model. *Tellus,* **41A,** 385-400.

Lindborg, E., 1999: Can the atmospheric kinetic energy spectrum be explained by two-dimensional turbulence? *J. Fluid Mech.,* **388,** 259-288.

Nastrom, G. D., and K. S. Gage, 1985: A climatology of atmospheric wavenumber spectra of wind and temperature observed by commercial aircraft. *J. Atmos. Sci.,* **42,** 950-960.

Skamarock, W. C., 2004: Evaluating Mesoscale NWP Models Using Kinetic Energy Spectra. *Mon. Wea. Rev.,* submitted. Available at *http://www.mmm.ucar.edu/individual/skamarock/ spectra_paper+figs.pdf*

Vallis, G. K., G. J. Schutts, and M. E. B. Gray, 1997: Balanced mesoscale motion and stratified turbulence forced by convection. *Q. J. R. Meteorol. Soc.,* **123,** 1621-1652.